JOURNAL OF PROPULSION AND POWER
Vol. 13, No. 3, May–June 1997

Stability Testing of Full-Scale Tactical Motors

F. S. Blomshield,* J. E. Crump,† H. B. Mathes,† and Richard A. Stalnaker‡
U.S. Naval Air Warfare Center, China Lake, California 93555
and
M. W. Beckstead§
Brigham Young University, Provo, Utah 84602

The U.S. Naval Air Warfare Center has participated in a program to develop an improved understanding of linear and nonlinear combustion instability in solid propellant rocket motors. One goal of this program was to develop a systematic database of motor and stability data. This paper describes the linear aspects of the motor firings and analysis. The motors that were used had diameters of 127 mm and were 1.7 m long. The majority were loaded with an 88% solids reduced-smoke ammonium perchlorate propellant with a nominal burning rate of 6.1 mm/s at 6.9 MPa. In addition, motors have been fired that contain 1% 8-μm aluminum oxide, 90-μm aluminum oxide, and 3-μm zirconium carbide as stability additives in place of 1% ammonium perchlorate. Motor pressures ranged from 3.45 to 10.34 MPa and various grain geometries were tested. Pressure-coupled combustion response measurements were made at the nominal motor operating pressures. Motor performance and stability calculations were made using the Air Force Solid Performance Program and the Standard Stability Prediction Program for the motor configurations that were fired. The stability predictions were compared to the data obtained from the motor firings. The results indicate that it is possible to theoretically predict linear motor stability for the class of motors discussed in this paper. It was also learned that higher-pressure motors tend to be less stable and that stability additives are very effective in controlling pulsed instabilities.

Introduction

A TOTAL of 23 motors were fired varying both motor configuration and propellant. The motor configurations are shown in Fig. 1. The baseline grain geometry was a six-point star in the aft two-thirds of the motor with a cylindrical section in the forward end. The motors were 1.7 m long with a diameter of 127 mm, giving them a length to diameter ratio of over 11. Ten of these baseline geometry motors were fired using the baseline reduced smoke propellant, NWR-11, and three were fired using propellants containing stability additives. Three motors with star-forward grains, one motor with a full star perforation, two motors with circular perforations, and four half-length motors were also fired.

The nomenclature used to identify the motors describes the geometry of the motors. The four grain geometries are star–aft (SAFT), star–forward (SFWD), full–star (SFUL), and cylinder (CYL). The length of the motor is designated as 3 or 6. The number 3 refers to the frequency of the first longitudinal mode for the full length motors (300 Hz) and the number 6 to the first mode frequency for the half-length motors (600 Hz). Thus, SAFT3 is a star-forward, full-length motor. The propellants used are designated with a Naval Weapons Research (NWR) number. Table 1 shows the complete motor test matrix. A complete documentation of the motor configurations, test conditions, instrumentation, and test results can be found in Ref. 1.

The baseline propellant (NWR-11) was an 88%-solids AP/HTPB propellant. The burning rate was 6.1 mm/s at 6.9 MPa and the burning rate exponent was 0.49. The propellant combustion response function was measured using the pulsed-during/pulsed-after burning T-burner technique.[2,3] The response curves for 3.45, 6.9, and 10.34 MPa are shown in Fig. 2. The zero-frequency condition was taken to be the burn rate exponent. A later mix of the NWR-11 formulation produced a low burning rate, designated as formulation NWR-11b in Table 1. Since the motor nozzle throats had been machined, all of the motors using NWR-11b propellant operated at a lower pressure than originally planned. Because of this, theoretical stability predictions of the NWR-11b motors will not be presented in this paper. They are discussed in Refs. 1 and 4.

Three motors were loaded with variations of the baseline propellant. One percent of the 55-μm ammonium perchlorate in the baseline propellant was replaced with a stability additive. The NWR-12 propellant contained 1% of 8-μm aluminum oxide, NWR-13 contained 1% of 3.5-μm zirconium carbide, and NWR-17 contained 1% of 90-μm aluminum oxide. The response function for the three propellants were determined from T-burner tests. They are shown in Fig. 3 along with the baseline propellant NWR-11. The additives also caused a slight shift in the propellant burning rate. Propellant properties have been summarized in Table 2. From Fig. 3 it can be seen that each of the additives lowered the response function by 25–35% below the baseline propellant over the frequency range of interest (300–1000 Hz).

Motor Predictions

The main thrust of the overall program was to develop an improved understanding of nonlinear (pulsed) combustion instability. Linear stability aspects were studied on this program because the nonlinear (pulsed) instability of a motor is believed related to its linear stability. The linear stability of a motor is characterized by its exponential decay (stability) or growth (instability) of pressure oscillations as follows:

$$\hat{P} = P_0 e^{\alpha t} \tag{1}$$

Received Feb. 12, 1991; presented as Paper 91-1954 at the AIAA/SAE/ASME/ASEE 27th Joint Propulsion Conference, June 24–26, 1991; revision received Jan. 30, 1997; accepted for publication Feb. 1, 1997.

*Research Scientist, Research and Technology Division. Senior Member AIAA.
†Research and Technology Division (Retired).
‡Research Technician, Research and Technology Division.
§Professor, Chemical Engineering Department. Associate Fellow AIAA.

Table 1 Motor test matrix

Test number	Geometry	NWR prop no.	Pressure, MPa	First mode frequency, Hz	Nozzle diameter, cm
1	SAFT	11	6.9	300	4.237
2	SAFT	11	6.9	300	4.237
3	SAFT	11	6.9	300	4.237
4	SFWD	11	6.9	300	4.237
5	SAFT	11	6.9	300	4.237
6	SAFT	11	3.45	300	4.699
7	FULL	11	6.9	300	4.267
8a	SAFT	11	6.9	300	4.267
8b	SAFT	11	3.45	300	4.699
8c	SAFT	11	10.34	300	3.708
8d	SAFT	11	6.9	300	4.237
9	CYL	11	6.9	300	4.001
10	CYL	11	3.45	300	4.343
11	SAFT	11b	6.9	600	3.048
12	SAFT	11b	10.34	600	2.870
13	CYL	11b	3.45	600	2.642
14	SFWD	11b	6.9	600	2.819
15	SAFT	12	6.9	300	4.237
16	SAFT	13	6.9	300	4.237
17	SAFT	17	6.9	300	4.237
19	SAFT	11b	13.79	300	3.429
20	SFWD	11b	6.9	300	4.237
21	SFWD	11b	6.9	300	4.237

Table 2 Additive propellants properties

Propellant no.	Additive	Size, μm	Rate,[a] cm/s	Response,[b] R_p	Exponent, n
NWR-11	(None)	——	0.605	1.25	0.491
NWR-12	Al_2O_3	8.0	0.630	0.75	0.493
NWR-13	ZrC	3.5	0.572	0.82	0.493
NWR-17	Al_2O_3	90.0	0.584	0.79	0.413

[a]Burning rate at 6.9 MPa. [b]Response function at 6.9 MPa and 300 Hz.

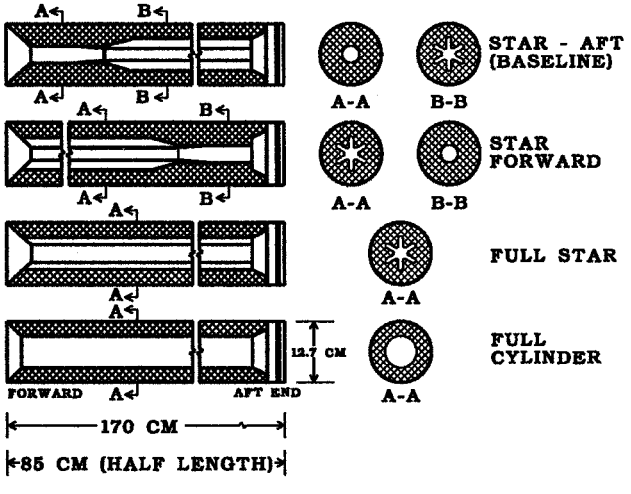

Fig. 1 Motor configurations.

The rate of growth (or decay) is expressed in terms of the alpha in this equation. If a pressure perturbation in the motor is damped, the alpha is negative and the motor is linearly stable. If the perturbation excites a growth of pressure oscillations, the alpha is positive and the motor is linearly unstable. Nonlinear instability, on the other hand, deals with the response to large or finite amplitude (nonlinear) types of disturbances.[5–9] Since knowledge of the linear stability was required, this facet of the program presented an opportunity to predict the linear stability of several motors and to make comparisons with linear experimental data that might be obtained under some test conditions. The Solid Propellant Performance

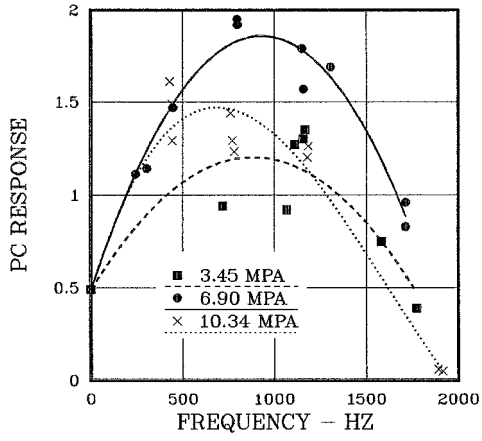

Fig. 2 Pressure-coupled combustion response of NWR-11 baseline propellant at 3.45, 6.9, and 10.34 MPa.

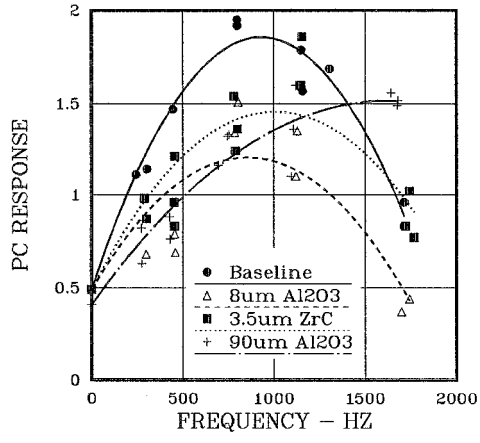

Fig. 3 Pressure-coupled response at 6.9 MPa of propellants containing stability additives.

Stability Prediction (SSP) computer program were used to predict the motor performance and linear stability of the baseline motor and all variations.[10,11]

Ballistics

One aspect of this study was developing the capability to predict the ballistic performance of a rocket motor using SPP.[10] A comparison of the measured pressure–time curve with the predicted curve for motor no. 5 is shown in Fig. 4. The initial prediction utilized a propellant strand burning rate determination over the pressure range of 1.38–13.79 MPa. After the motor firing the burning rate was adjusted to give the correlation shown in Fig. 4. The burning rate used in the correlation was 6.1 mm/s at 6.9 MPa. The large ignition spike and large tailoff are both indicative of erosive burning in the motor. The erosive burning parameters in SPP also had to be adjusted extensively to match the ignition spike and tailoff.

An example of the mean pressure for a motor that was pulsed unstable is shown in Fig. 5 along with predicted steady-state pressure. The pressure trace is from motor no. 4, which was a full-length star-forward geometry operating at a nominal pressure of 6 MPa. The high pressure during the oscillating portion of burning (i.e., the dc pressure shift) was because of the acoustic erosivity associated with oscillatory combustion. It should be noted that the motor was pulsed at 0.97 s at an amplitude of 207 kPa or 4%, and the motor was stable to that pulse for that geometry. The second pulse was at 1.96 s at an amplitude of 152 kPa or 2.5%, which was sufficient to trigger the observed nonlinear combustion instability. It is significant

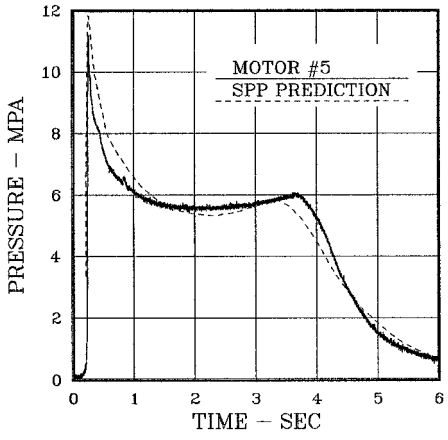

Fig. 4 Comparison of predicted and measured pressure–time curves for star-aft 300-Hz motor 5.

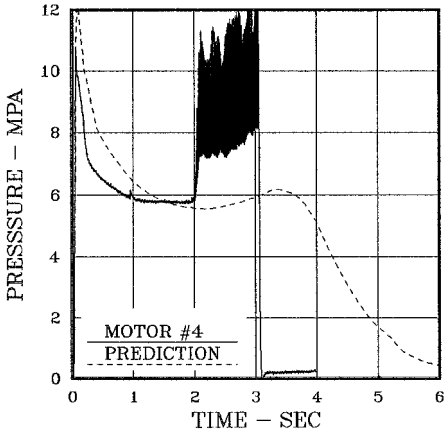

Fig. 5 Comparison of predicted and measured pressure–time curves for star-forward 300-Hz motor 4 (unstable).

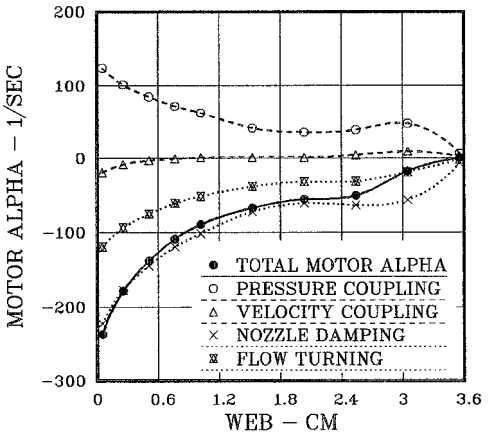

Fig. 6 Stability prediction for star-aft configuration (300 Hz) at 6.9 MPa.

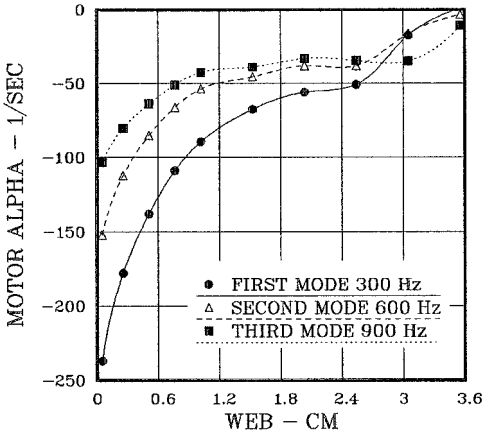

Fig. 7 Stability prediction for star-aft configuration (300 Hz) at 6.9 MPa for first three axial acoustic modes.

to note (and is discussed more in a companion paper[12]) that a smaller pulse will trigger instability later in firing because of an increased volume and a reduced mean flow velocity.[1]

Stability Predictions

The SSP method was used to predict the linear stability of the baseline motor and all variations.[11,13,14] The linear stability elements (expressed as growth and decay alphas) for the baseline motor are shown in Fig. 6. The algebraic sum of the pressure-coupled (PC) alpha, the velocity-coupled (VC) alpha, the nozzle damping (NOZ), and the flow-turning damping (FT) yields the motor alpha (MOTOR). If the sum is negative, the motor is said to be linearly stable, i.e., it is stable to small pressure disturbances. If the sum is positive, the motor is said to be spontaneously unstable, i.e., minute pressure oscillations will grow. The measured pressure-coupled response function of the propellants was an input to calculate the pressure coupling in the motors. The velocity-coupled response was not measured but was set to unity. It is considered unimportant because the integral for velocity coupling over the waveform was computed to be very small for the motor configurations in this study. Thus, for high L/D motors, velocity coupling can be considered as negligible. From the figure it is evident that there are three mechanisms that are significant for this propellant–motor system: 1) pressure coupling, 2) flow turning, and 3) nozzle damping. The pressure coupling and the flow turning essentially counterbalance each other and the margin of stability decreases as the volume increases.

Since nonlinear stability involves steep-fronted pressure waves (multiple acoustic mode frequencies), the linear stability of the higher longitudinal acoustic modes of the baseline motor is of interest. The motor alphas for the first three modes of the baseline motor at 6.9 MPa are shown in Fig. 7. The higher modes have lower linear stability limits (smaller absolute values of the motor alpha) than the first longitudinal mode (300 Hz) and may be responsible for the susceptibility of the motor to pulsing. This is the result of the propellant response function increasing with increasing frequency over the frequency range of 300–1000 Hz (Fig. 2). The pulse contains relatively high-frequency components that tend to excite higher frequency modes of the motor. The fact that the higher frequency modes are less stable linearly may promote the nonlinear response of the motor to a pulse.

Motor Test Data

All of the motors in this program were instrumented with at least one ballistic pressure transducer and two closely coupled high-frequency response pressure transducers located in the forward end of the motor. Details of the instrumentation are found in Refs. 1, 15, and 16.

The motors tested, the planned pulsing, and the qualitative test results are indicated in Table 3. The pulsing of motors 11–14 and motors 19–21 was intended to get three pulse decays that would provide data for more correlations with linear stability predictions. The intent with motors 15–18 was to pulse them in the same manner as the baseline motors to see if the additives had an effect on nonlinear instability.

Data from motors that were pulsed but remained stable was analyzed to determine the linear motor stability margin. This was done by measuring the decay rate of the pressure oscillations (motor alpha) following the pulse. Table 3 lists the motor pressure P_{av}, pulse times, web, pulse amplitudes, and

Table 3 Pulse time-amplitude-alpha comparison

Test no.	Geometry	P_{ave}, MPa	NWR prop no.	Pulse no. 1 Time, s	Web, cm	Pulse, kPa	α, 1/s	Pulse no. 2 Time, s	Web, cm	Pulse, kPa	α, 1/s	Pulse no. 3 Time, s	Web, cm	Pulse, kPa	α, 1/s
1	SAFT3	5.52	11	NRD[a]	——	——	——	2.016	1.270	248	+209	OSC[b]	——	——	——
2	SAFT3	5.52	11	0.703	0.503	83	−159	1.708	1.092	83	+207	OSC[b]	——	——	——
3	SAFT3	5.52	11	0.805	0.566	97	−112	1.790	1.240	345	+161	OSC[b]	——	——	——
4	SFWD3	6.21	11	0.970	0.864	262	−190	1.962	1.506	152	+56	OSC[b]	——	——	——
5	SAFT3	5.52	11	0.965	0.660	690	−176	NPF[c]	——	——	——	NPF[c]	——	——	——
6	SAFT3	3.72	11	0.760	0.467	124	−214	2.005	1.092	48	−102	3.010	1.549	41	−75
7	SFUL3	6.21	11	0.748	0.640	262	+639	OSC[b]	——	——	——	OSC[b]	——	——	——
8a	SAFT3	5.52	11	NPF[c]	——	——	——	NPF[c]	——	——	——	3.020	1.816	69	+134
8b	SAFT3	3.72	11	0.950	0.559	345	−210	2.216	1.181	138	−89	3.419	1.732	221	+366
8c	SAFT3	10.3	11	0.617	0.538	138	+151	OSC[b]	——	——	——	OSC[b]	——	——	——
8d	SAFT3	5.52	11	NPF[c]	——	——	——	NPF[c]	——	——	——	NPF[c]	——	——	——
9	CYL3	5.72	11	0.745	0.351	138	+232	OSC[b]	——	——	——	OSC[b]	——	——	——
10	CYL3	4.21	11	0.887	0.406	248	+244	OSC[b]	——	——	——	OSC[b]	——	——	——
11	SAFT6	3.31	11b	2.067	0.815	276	−143	3.688	1.445	41	−75	5.218	2.507	28	−60
12	SAFT6	5.52	11b	1.374	0.599	83	−182	2.543	1.102	41	−247a[d]	NRD[a]	——	——	——
13	CYL6	4.00	11b	1.261	0.442	55	−185	2.429	0.902	28	NRD	3.445	1.334	28	−71
14	SFWD6	4.55	——	1.945	0.930	345	−201	3.465	1.631	55	−133	4.898	2.319	14	−33a[d]
15	SAFT3	6.48	12	0.948	0.719	1200	−122	1.764	1.242	276	−84	NRD[a]	——	——	——
16	SAFT3	4.96	13	0.824	0.533	359	−232	1.505	0.899	179	−137	NRD[a]	——	——	——
17	SAFT3	5.72	17	0.866	0.579	483	−188	1.660	1.044	317	−75	2.572	1.542	14	−110a[d]
19	SAFT3	10.1	11b	NRD[a]	——	——	——	1.817	1.247	14	−26a[d]	2.767	1.842	14	−64a[d]
20	SFWD3	5.03	11b	0.984	0.752	110	−193	2.167	1.402	28	−81	NPF[c]	——	——	——
21	SFWD3	5.03	11b	1.012	0.770	290	−251	2.195	1.417	69	−143	3.506	2.060	28	NRD[a]

[a]Not reducible. [b]Oscillating. [c]No pulse fired. [d]Weak pulse actual pulse amplitude determined by extrapolated back to zero time.[1,12,15,16]

decay alphas. As shown in Table 3 some of the motors were stable to the pulses. Some of those pulses were very weak and resulted in situations where the pulse was too small to detect in the data or too small to give meaningful decay alphas because of the poor signal-to-noise ratio.

Linear Correlations

Mean Pressure Comparison

Motors 1–6 were fired in the first test series. A total of three pulses decayed in motors 2, 3, and 5. The pulse decay rates are plotted in Fig. 8 along with the linear stability prediction for the fundamental frequency for that configuration at 6.9 MPa. A total of five pulse decays were also measured in motors 6 and 8b. These are also plotted in Fig. 8 along with the linear prediction for 3.45 MPa. The agreement between the measurements and the predictions is very good. It is particularly significant that the motor becomes less stable during the firing and both the calculations and data show this trend. This is because of the increase in motor volume as the propellant burns out, with alpha being inversely proportional to the motor volume. It is also worth noting that the lower-pressure motor was more stable than the higher-pressure motor. The greater stability of the lower-pressure motor is because of less driving (a lower response function, Fig. 2), greater nozzle damping because of a larger nozzle diameter, and more flow turning losses because of a greater mean flow velocity. Table 4 shows individual alphas and total alphas predicted by the SSP program for these two motor pressures.

In the past, the validity of the flow-turning term included by Culick has been questioned.[12,13] In all of the calculations in this paper the flow turning has been included and the agreement between the data and the calculations is reasonable. This would seem to give, at least, qualitative credence to the concept of flow turning.

Additive Propellants

Motors 15, 16, and 17 were loaded with propellants containing stability additives. The propellants with additives had burning rates that were somewhat different than the baseline propellant, NWR-11. Table 2 shows some of the properties of the propellants. Because of the differences in burning rates (and the use of standard nozzles), the ballistic behavior of the

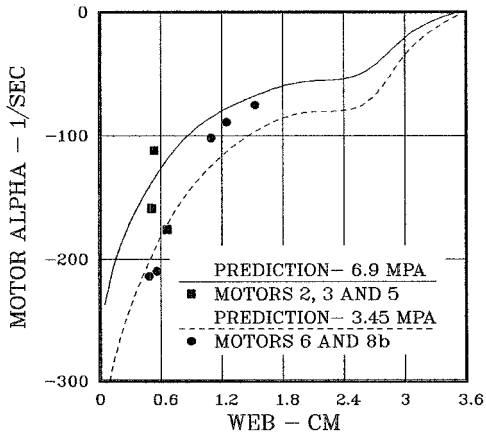

Fig. 8 Measured and predicted star-aft 300-Hz motor alphas for motors 2, 3, and 5 (6.9 MPa) and motors 6 and 8b (3.45 MPa).

motors was different than originally planned. These differences are reflected in the pressure–time curves shown in Fig. 9. The results of the linear stability calculations are shown in Fig. 10. The motor stability margins for all of the motors with additives are virtually the same and are significantly greater than the stability margin for the baseline motor. The computed particle damping is very small (less than five reciprocal seconds) at these frequencies. The increased stability is because of the lower response functions of the additive-containing propellants (refer to Fig. 3).

If one looks at the stability margins for the additive propellants in greater detail (Fig. 11), it is seen that the motor using NWR-13 propellant had the largest stability margin. One might expect that the propellant with the smallest value of the propellant response function would have the greatest margin (NWR-12, Table 2). However, in this comparison, the ballistics of the three additive motors were different because of the slight burning rate differences (Fig. 9). Hence, the changes (increases) in the other factors that make up the motor stability margin (mainly, the changes in the mean flow velocity) were greater than the change (decrease) in the pressure-coupled alpha because of the decrease in the response function for the

Table 4 Individual alphas for 3.45- and 6.9-MPa star-aft geometries

Web, cm	Total alpha		PC response		VC response		Nozzle damping		Flow turning	
	3.45	6.9	3.45	6.9	3.45	6.9	3.45	6.9	3.45	6.9
0.051	−319	−237	104	123	−23	−20	−261	−222	−140	−119
0.254	−250	−178	88	102	−10	−8	−214	−177	−114	−94
0.508	−197	−138	74	85	−4	−3	−175	−144	−92	−75
0.762	−157	−109	63	72	−1	−1	−145	−119	−75	−61
1.016	−131	−89	55	63	1	1	−124	−102	−63	−52
1.524	−97	−67	37	42	2	1	−88	−72	−47	−38
2.032	−81	−56	31	36	2	1	−75	−61	−39	−32
2.540	−77	−51	35	40	6	5	−78	−64	−39	−31
3.048	−30	−18	34	48	10	9	−55	−57	−18	−19
3.556	−1	1	5	7	3	3	−7	−7	−1	−1

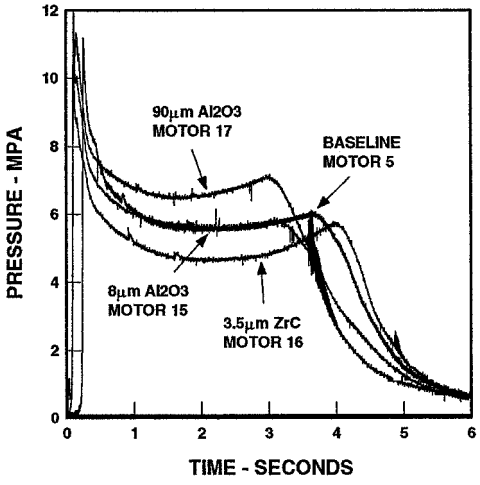

Fig. 9 Pressure–time curves for star-aft 300-Hz motors with propellant additives.

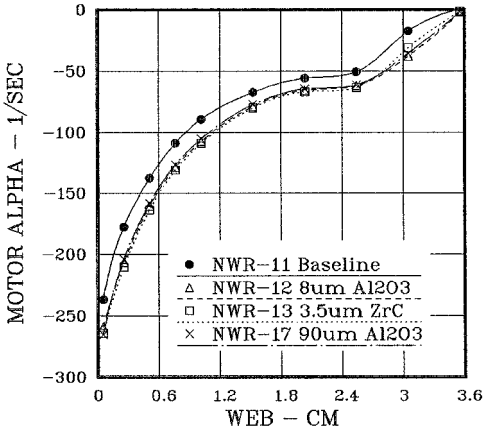

Fig. 10 Stability predictions for star-aft 300-Hz motors with additives at 6.9 MPa.

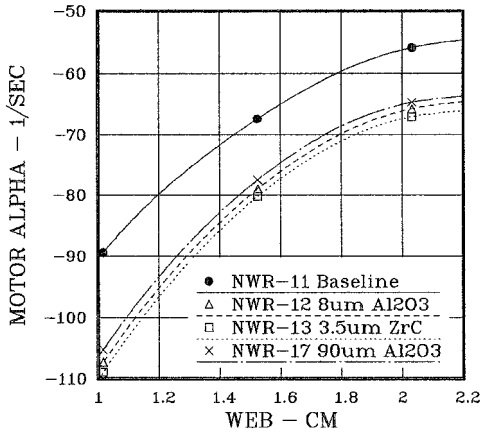

Fig. 11 Enlarged view of stability predictions for motors with additives.

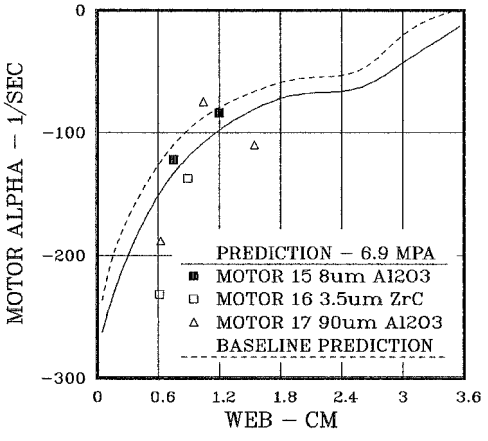

Fig. 12 Measured and predicted motor alphas for additive motors 15, 16, and 17 (6.9 MPa) and prediction of baseline motor.

additive propellant motor firings. The point to be made here is that in the motor geometry–propellant system a decrease in the propellant response function does not necessarily result in an increase in the motor stability margin.

Pulse decay rates for the first, second, and third pulses in the three additive motors were measured and compared to the linear stability prediction. These comparisons are shown in Fig. 12. The trend of the data is, again, in agreement with the prediction. The predicted linear stability margin for the baseline motor is shown for comparison. The stability margin for the baseline propellant is considerably less, primarily because it does have a significantly higher-pressure coupled response (see Table 2 and Fig. 3). Table 5 shows the individual alphas and the total alphas predicted by the SSP program representative of the additive motors using NWR-12 propellant and the baseline propellant motor.

The principle intent with motors 15–17 was to pulse them in the same manner as the baseline motors to see if the additives had an effect on nonlinear instability. Unfortunately, the strengths of the first pulses for motors 15–17 (1200, 359, and 483 kPa or 20, 6, and 8%) were not, in general, comparable to the first pulses of the baseline propellant for motors 2, 3, and 5 (83, 97, and 690 kPa or 1.4, 1.6, and 11%) (see Table 3). However, the fact that these motors remained stable to more severe pulses than the baseline motor is significant. This suggests the powerful role stability additives can play in combustion instability suppression. For the second pulses, if one considers the pulse amplitudes on the additive motors 15, 16, and 17 (276, 179, and 317 kPa or 4.7, 3.0, and 5.3%) to be nearly comparable to the second pulse in motors 1, 2, and 3 (248,

Table 5 Individual alphas representative of the three additive motors using NWR-12 propellant and the baseline propellant motor at 6.9 MPa and 300 Hz with the star-aft geometry

Web, cm	Total alpha		PC response		VC response		Nozzle damping		Flow turning		Part damping[a]	
	Additive	Baseline	Additive	Baseline	Additive	Baseline	Additive	Baseline	Additive	Baseline	Additive	Baseline
0.051	−263	−237	68	123	−17	−20	−202	−222	−110	−119	−2.3	0
0.254	−210	−178	58	102	−8	−8	−167	−177	−89	−94	−2.4	0
0.508	−164	−138	48	85	−3	−3	−135	−144	−72	−75	−2.4	0
0.762	−132	−109	41	72	0	−1	−111	−119	−58	−61	−2.4	0
1.016	−110	−89	35	63	1	1	−95	−102	−49	−52	−2.4	0
1.524	−82	−67	24	42	1	1	−68	−72	−37	−38	−2.4	0
2.032	−68	−56	20	36	1	1	−57	−61	−30	−32	−2.5	0
2.540	−65	−51	22	40	4	5	−59	−64	−29	−31	−2.5	0
3.048	−41	−18	29	48	9	9	−57	−57	−19	−19	−2.4	0
3.556	−13	1	4	7	3	3	−7	−7	−1	−1	−2.4	0

[a] This particle damping assumes 1% 8-μm Al_2O_3.

Table 6 Individual alphas for star-forward motor 4 and star-aft baseline geometry at 6.9 MPa and 300 Hz

Web, cm	Total alpha		PC response		VC response		Nozzle damping		Flow turning	
	Star-forward	Star-aft	Star-forward	Star-aft	Star-forward	Star-aft	Star-forward	Star-aft	Star-forward	Star-aft
0.051	−311	−237	108	123	−22	−20	−272	−222	−125	−119
0.254	−249	−178	93	102	−15	−8	−230	−177	−97	−94
0.508	−199	−138	78	85	−10	−3	−191	−144	−77	−75
0.762	−159	−109	66	72	−7	−1	−157	−119	−61	−61
1.016	−132	−89	57	63	−5	1	−133	−102	−51	−52
1.524	−99	−67	39	42	−4	1	−96	−72	−39	−38
2.032	−80	−56	33	36	−2	1	−78	−61	−32	−32
2.540	−60	−51	25	40	−4	5	−57	−64	−24	−31
3.048	−24	−18	19	48	−5	9	−29	−57	−9	−19
3.556	−5	1	6	7	−3	3	−7	−7	−1	−1

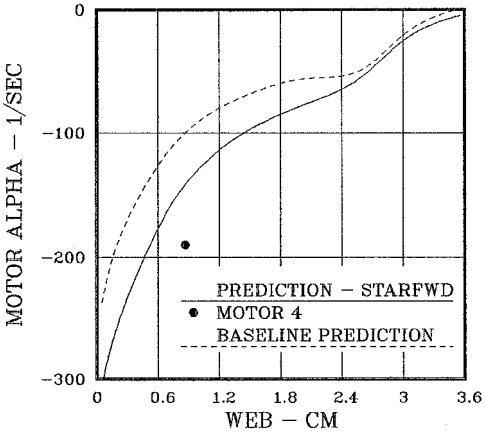

Fig. 13 Measured and predicted star-forward 300-Hz motor alpha for motor 4.

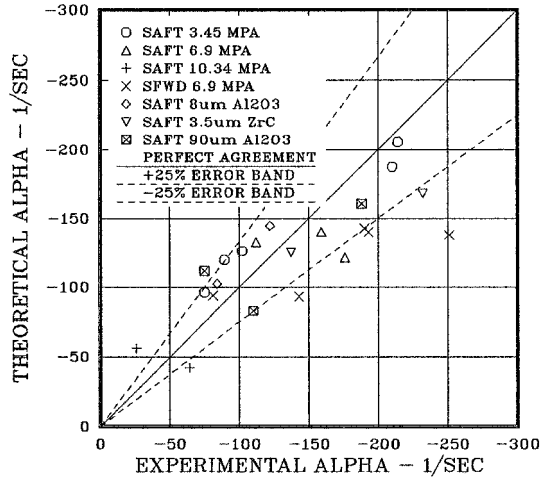

Fig. 14 Measured vs theoretical decay alphas for all motors.

83, and 345 kPa or 4.2, 1.4, and 5.8%), one could conclude that the additives did increase the margin of stability since the pulses in the additive motors decayed while the pulses in motors 1, 2, and 3 grew. The lower value of the response function for the higher modes for the additive propellants supports this conclusion (see Fig. 3), since a pulse could not as easily excite these modes into a nonlinear instability. Particle damping also contributes to the observed behavior. The particle damping computed for the first longitudinal mode is very low, as can be seen in Table 5. However, the particle damping will be more effective for the higher modes and will help damp out oscillations at the higher modes, lessening the likelihood of nonlinear instability. There is only one data point to compare for the third pulse. The stable third pulse of motor 17 (14 kPa or 0.23%) and the unstable third pulse of motor 8a (69 kPa or 1.2%). Although no definite conclusion can be made from this third pulse comparison, it is consistent with the previous conclusions.

Geometry Variations

The primary purpose of motors 4, 20, and 21 was to obtain additional linear stability data for correlation with the linear stability predictions and examine geometric effects. These motors were cast with the star-forward grain configuration. Unfortunately, motors 20 and 21 were cast with the low-rate propellant mix, NWR-11B. The single decay rate for motor 4 was measured and is plotted in Fig. 13 for comparison with the linear stability calculations. The solid circle on the plot is the decay alpha measured for motor 4. It is to be compared to the solid line prediction. Also shown in Fig. 13 is the predicted stability for the baseline star-aft geometry (dashed line). The single data point in Fig. 13 is in fairly good agreement with the prediction. The increase in stability for the star-forward geometry is caused by an increase in the nozzle damping because of the smaller port areas at the aft end of the motor. Table 6 shows the individual alphas and the total alphas pre-

dicted by the SSP program for these two motor lengths using the baseline normal rate propellant. The other two geometries fired in the program (full star motor number 7 and full cylinder motor number 9) yielded no stable pulses, so that no linear comparisons could be made. The SSP calculations showed the cylinder geometry to be the least stable, the star aft and full star comparable, and the star forward to be the most stable. It is unfortunate that a comparison could not be made with the data. However, the fact that both of the axially symmetric geometries became unstable may indicate that axial symmetric geometries are more susceptible to pulsed instability.

Summary of Linear Stability Comparisons

Figure 14 shows all of the measured decay alphas vs the theoretically predicted decay alphas. The plot is marked according to motor pressure, length, propellant, and geometry. Twenty-five percent error bands are also shown. Most of the comparisons fall within the error bands.

Conclusions

The ballistic pressure–time curves for most of the motors in this program were satisfactorily predicted by the Solid Performance Program. In many cases the actual values of measured stability were correctly predicted. In all cases the trends in measured stability were confirmed by the Standard Stability Program. Perhaps the most important input for the program (and one of the most difficult to determine) is the correct pressure-coupled response function for the propellant. Also, critical for accurate stability analysis, is the correct burning rate of the propellant in the motor.

Effects of pressure, motor length or frequency, additives, and geometry were all examined. The pressure effect that was predicted and validated with data showed that increasing pressure reduces the margin of stability in this case. The effect of stability additives on nonlinear stability was significant. The data indicated that stability additives were effective in increasing the nonlinear stability margin. However, differences between different stability additives were not evident. Finally, motor geometry comparisons were made that indicated that a star–forward geometry was more stable than a star–aft geometry. This conclusion was validated both experimentally and theoretically. In addition, the constant cross-sectional geometries (full–star and full–cylinder) were observed to be very sensitive to pulsing and resulting instabilities.

References

[1]Blomshield, F. S., Crump, J. E., Mathes, H. B., and Beckstead, M. W., "Stability Testing and Pulsing of Full Scale Tactical Motors," Naval Air Warfare Center, Weapons Div., NAWCWPNS-TP-8060, July 1993.

[2]Crump, J. E., "Combustion Instability of Minimum Smoke Propellants, Part 1. Experimental Techniques and Results," Naval Air Warfare Center, Weapons Div., NAWCWPNS TP 5936, Nov. 1977.

[3]"T-Burner Manual," Chemical Propulsion Information Agency, Publication 191, Nov. 1969.

[4]Blomshield, F. S., Crump, J. E., Mathes, H. B., and Beckstead, M. W., "Stability Testing of Full Scale Tactical Motors," AIAA Paper 91-1954, June 1991.

[5]Brownlee, W. G., "Non-Linear Axial Combustion Instability in Solid Propellant Motors," *AIAA Journal*, Vol. 2, No. 2, 1964, pp. 275–284.

[6]Jensen, R. C., and Beckstead, M. W., "Limiting Amplitude Analysis," Hercules, Inc., AFRPL-TR-73-61, Magna, UT, July 1973.

[7]Baum, J. D., Levine, J. N., and Lovine, R. L., "Pulse-Triggered Instability in Solid Rocket Motors," *AIAA Journal*, Vol. 22, No. 10, 1984, pp. 1413–1419.

[8]Baum, J. D., and Levine, J. N., "Modeling of Nonlinear Longitudinal Instabilities in Solid Rocket Motors," *Acta Astronautica*, Vol. 13, Nos. 6, 7, 1984, pp. 339–348.

[9]Baum, J. D., Levine, J. N., and Lovine, R. L., "Pulsed Instability in Rocket Motors: A Comparison Between Predictions and Experiments," *Journal of Propulsion and Power*, Vol. 4, No. 4, 1988, pp. 308–316.

[10]Hermsen, R. W., Lamberty, J. T., and McCormick, R. E., "A Computer Program for the Prediction of Solid Propellant Rocket Motor Performance (SPP)," Vol. V, AFRPL-TR-84-036, Sept. 1984.

[11]Nickerson, G. R., Culick, F. E. C., and Dang, L. D., "Standard Stability Prediction Program for Solid Rocket Motors," Air Force Rocket Propulsion Lab., TR-83-017, Sept. 1983.

[12]Blomshield, F. S., Mathes, H. B., Crump, J. E., and Beiter, C. A., "Nonlinear Stability Testing of Full-Scale Tactical Motors," *Journal of Propulsion and Power*, Vol. 13, No. 3, 1997, pp. 356–366.

[13]Culick, F. E. C., "Stability of Longitudinal Oscillations with Pressure and Velocity Coupling in a Solid Propellant Rocket," *Combustion Science and Technology*, Vol. 2, 1970, pp. 179–201.

[14]Culick, F. E. C., "The Stability of One-Dimensional Motions in a Rocket Motor," *Combustion Science and Technology*, Vol. 7, 1973, pp. 165–175.

[15]Blomshield, F. S., Beiter, C. A., Mathes, H. B., Crump, J. E., and Beckstead, M. W., "Non-Linear Stability Testing and Pulsing of Full Scale Tractical Motors," AIAA Paper 91-1953, June 1991.

[16]Blomshield, F. S., Jolley, W. H., Harris, P. G., and Tandy, I. F. S., "The Technical Cooperation Program Technical Panel W-4: Propulsion Technology, KTA-11: Pulsed Non-Linear Combustion Instability," Vols. I–VI, The Technical Cooperation Program Final Rept., U.S. Naval Weapons Center, China Lake, CA, Oct. 1991.